



August 17, 2017

PG&E Letter DCL-17-070

U.S. Nuclear Regulatory Commission  
ATTN: Document Control Desk  
Washington, DC 20555-0001

Docket No. 50-275, OL-DPR-80  
Diablo Canyon Unit 1  
Flaw Evaluation of Unit 1 Residual Heat Removal Suction Weld Joint

References:

1. PG&E Letter DCL-17-049, "Flaw Evaluation of Unit 2 Residual Heat Removal Suction Weld Joint," dated May 18, 2017
2. PG&E Letter DCL-17-048, "Request for Approval of an Alternative to the American Society of Mechanical Engineers (ASME) Boiler and Pressure Vessel Code Section XI Examination Requirements for Class 1 and 2 Piping Welds," dated May 18, 2017

Dear Commissioners and Staff:

In accordance with the requirements of the American Society of Mechanical Engineers (ASME) Boiler and Pressure Vessel Code (BPVC) Section XI, 2007 Edition through 2008 Addenda, Paragraphs IWB-3132.3, IWB-3134(b), and IWB-3640, Pacific Gas & Electric Company (PG&E) is submitting the results of the analytical evaluation of a flaw found in Diablo Canyon Power Plant Unit 1, on the 14-inch diameter ASME Code Class 1 weld identified as WIB-228. IWB-3134(b) states, "Analytical evaluation of examination results as required by IWB-3132.3 shall be submitted to the regulatory authority having jurisdiction at the plant site."

PG&E identified a circumferential indication in the Unit 1 Residual Heat Removal (RHR) suction pipe at weld joint WIB-228. The indication was found using ultrasound examination techniques during an extent of condition inservice inspection performed during the Unit 1 twentieth refueling outage. WIB-228 is the pipe-to-45 degree elbow weld on the wrought stainless steel RHR hot leg suction pipe inside the containment building downstream of the Loop 4 reactor coolant system hot leg branch connection. The weld/pipe location in Unit 1 is similar to the weld/pipe location in Unit 2, where a weld flaw was found (Reference 1).

The flaw exceeds the acceptance standards of ASME BPVC Section XI, 2007 Edition through 2008 Addenda, Table IWB-3514-2. The flaw was initially dispositioned as unacceptable. Subsequently, an analytical evaluation was performed based on the rules of ASME BPVC Section XI, Paragraph IWB-3640.



The evaluation concluded that the weld containing the flaw is acceptable for continued service for Cycle 21 operation, which will not exceed two years. The analytical evaluation that was performed for Unit 2 (Reference 1) was replicated using the flaw parameters, pipe dimensions, and loads that are applicable to Unit 1. The specific mechanisms considered were thermal shock from cyclic swirl penetration and cyclic thermal stratification, and stress corrosion cracking (SCC). Available pipe surface temperatures from Unit 2 thermocouple monitoring data were used to perform the analytical evaluation for Unit 1, since the configuration of the pipe/weld, materials, operation, and load history are similar for both Units 1 and 2. Vibration was ruled out as a possible cause based on the inspections performed by PG&E, which concluded that the physical evidence indicative of excessive vibration was not present.

Because the evaluation could neither rule out nor specify the specific flaw growth mechanism, a conservative analysis was performed combining the effects of two different flaw growth mechanisms: fatigue crack growth and SCC. The results of this conservative analysis were used to justify continued operation of Unit 1 for an additional cycle. However, PG&E is not attributing SCC with respect to risk-informed inservice inspection (RI-ISI) weld inspections requested by Reference 2 due to uncertainty regarding the flaw growth mechanism.

The results of the analysis show that it would take 35 months for the as-found flaw depth of 0.2 inch to reach the allowable flaw size using the most limiting crack growth rate. Therefore, the continued operation of Unit 1 for an additional cycle was determined to be acceptable. The analysis, methodology, and results are provided in the Enclosure.

PG&E makes no new or revised regulatory commitments (as defined by NEI 99-04) in this letter. If you have any questions or require additional information, please contact Mr. Hossein Hamzehee at (805) 545-4720.

Sincerely,

James M. Welsch  
*Vice President, Nuclear Generation*

rnrt/4231/50915871-26  
Enclosure



Document Control Desk  
August 17, 2017  
Page 3

PG&E Letter DCL-17-070

cc: Diablo Distribution  
cc/enc: Scott A. Morris, NRC Region IV Administrator (Acting)  
Christopher W. Newport, NRC Senior Resident Inspector  
Gonzalo L. Perez, Branch Chief, California Department of Public Health  
Balwant K. Singal, NRC Senior Project Manager  
State of California, Pressure Vessel Unit

**Diablo Canyon Power Plant, Unit 1**

**Residual Heat Removal (RHR) Piping Flaw Evaluation Report**

August 04, 2017  
Report No. 1700609.401.R1  
Quality Program:  Nuclear  Commercial

Mr. Mark Sharp  
Pacific Gas and Electric Company  
Diablo Canyon Power Plant  
PO Box 56  
Avila Beach, CA 93424

Subject: Diablo Canyon Power Plant Unit 1 Residual Heat Removal (RHR) Piping Flaw Evaluation

Dear Mark:

In response to your request dated 5/1/17, this report documents the flaw evaluation of the recently discovered flaw in the RHR Suction Weld Joint at Diablo Canyon Power Plant (DCPP) Unit 1.

## BACKGROUND

During the scheduled refueling outage 1R20 work, ultrasound (UT) inspection on Unit 1 weld WIB-228 identified an ultrasonic reflector at approximately 01:00 on 4-28-17 [15]. This is line 109 of the RHR system "Hot Leg Recirc Before Isolation Valve V-8702." This weld is a pipe-to-45° elbow off the Loop 4 hot leg (see Figure 1). This is the same weld/pipe location in Unit 2 (WIB-245) where a weld flaw was found in 2R19.

The objective of this report is to perform a flaw evaluation for the flaw found in Unit 1 weld WIB-228 using two flaw growth mechanisms of fatigue and stress corrosion cracking (SCC) to justify continued operation for an additional cycle.

Since the flaw was found at a similar location as Unit 2, the flaw evaluation performed for Unit 2 is replicated using the flaw parameters, pipe dimensions, and loads applicable to Unit 1. Based on the conservative treatment of loading uncertainties in the analyses performed for Unit 2 [1], SI recommended the application of temporary thermocouples to both welds of the 45° elbow to better understand the real loading. The temperature monitoring conducted by DCPD for Unit 2

Toll-Free 877-474-7693

was implemented by attaching thermocouples to the outside surface of the piping at several locations as shown in Figure 2. A revised analysis for Unit 2 was performed using the thermocouple data [2] to more accurately calculate the thermal stresses. This data shows that the RHR has cyclic stratification of the unisolable horizontal pipe section. This data allowed for the calculation of more accurate local stresses and global bending loads due to stratification and thermal expansion. Since the configuration of the pipe/weld, materials, operation and load history are similar for both Units 1 and 2, the available Unit 2 thermocouple data is used to perform the flaw evaluation for Unit 1. Note that the cracking found in Unit 1 is not as severe as the cracking found in Unit 2. Vibration was not included since it was ruled out as a possible cause.

This report documents the loads used to calculate stresses and stress intensity factors to determine crack growth (from both fatigue and SCC) and the allowable flaw size. Based on the evaluation contained herein, the flawed component is acceptable for continued operation. The flaw is not expected to exceed the ASME Code, Section XI allowable flaw size for the next 35 months.

## DESIGN INPUT

### Geometry

Pipe outside diameter (OD) = 14 inches [3]

Pipe thickness = 1.406 inches [3]

### Loads

The flaw location is shown in Figure 1 and is at Node 503 per Reference [3]. All piping loads are obtained from Reference [3] at Node 503 and are shown in Figure 3.

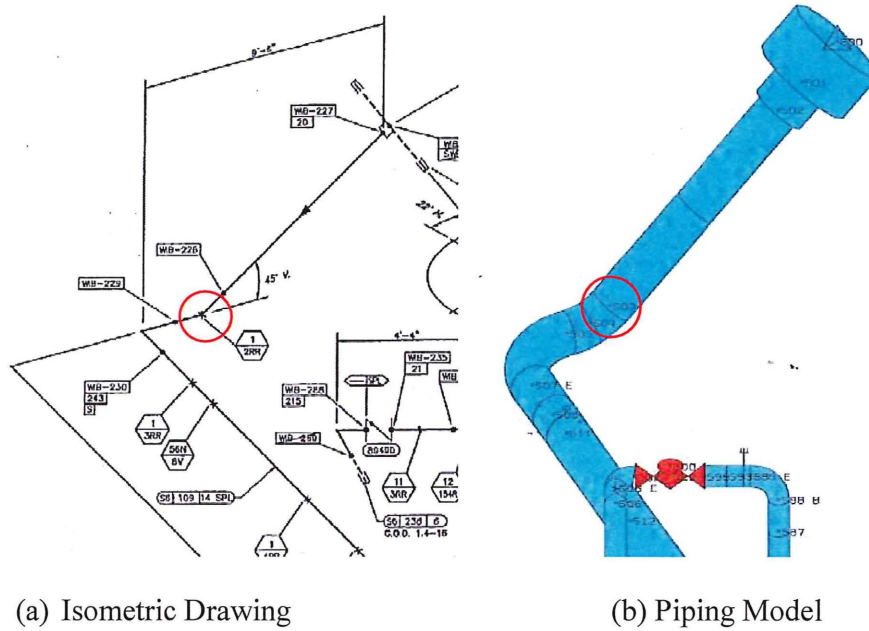


Figure 1. Flaw Location

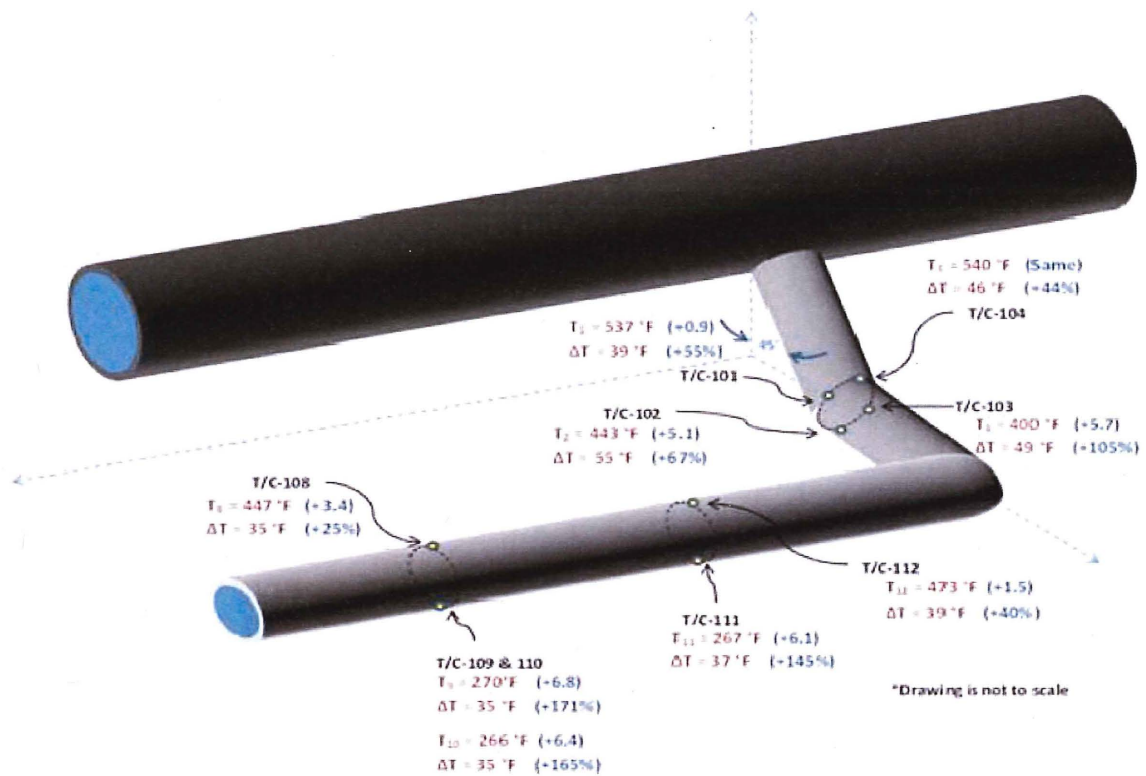
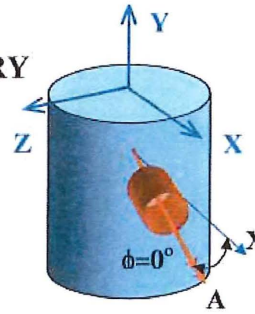


Figure 2. RHR Piping Thermocouple Locations for Unit 2

**NOZZLE LOAD SUMMARY**  
 FOR CLASS 1 EQUIPMENT

PIPE ELEMENT 502 - 503  
 Load @ Node #503



NODE NO. : 503                      MFID : 2H4256  
 NOZZLE ID:                      P&ID DWG. NO.: 102007  
 PIPING SYSTEM : RHR - RCS SYSTEM                      LINE NUMBER : S6-109-14  
 EQUIPMENT NAME : PIPE - ELBOW  
 COSAX, COSAY, COSAZ : -0.265 -0.707 0.656  
 COSBX, COSBY, COSBZ : 0.265 -0.707 -0.656  
 COSCX, COSCY, COSCZ : 0.927 0.000 0.375  
 LOADS GIVEN AT [ ] SHELL [ ] NOZZLE FLANGE

LOADING CONDITION	FORCE (LBS)			MOMENT (FT-LBS)		
	FA	FB	FC	MA	MB	MC
<b>DEADWEIGHT:</b>						
DL	-197.	-107.	0.	1194.	-1380.	-1440.
<b>THERMAL:</b>						
THRMN1	641.	-1513.	-2458.	22737.	-3949.	1118.
THRMN2	672.	-1571.	-2572.	23590.	-4267.	1307.
THRMN3	1461.	-653.	-1740.	23167.	14469.	6200.
THRMN4	984.	-417.	-1195.	18332.	7875.	5400.
THRMN5	-124.	55.	110.	1021.	-3026.	545.
THRMN6	375.	-720.	-1265.	12562.	-935.	988.
THRMA1	888.	-920.	-2261.	23395.	-3911.	6549.
THRMA2	966.	-1153.	-2584.	23575.	-4141.	6033.
THRMA3	635.	-99.	-630.	11600.	5973.	3948.
THRMA4	716.	-378.	-1011.	12484.	6789.	2809.
THRMA5	133.	-1635.	-1612.	30459.	-5678.	632.
THRMA6	215.	-1914.	-1993.	31343.	-4862.	-507.
<b>SEISMIC-INERTIA:</b>						
DE	990.	1882.	1330.	2642.	1962.	2560.
DDE	1622.	2841.	1795.	3543.	2958.	4021.
HOSGRI	2220.	5197.	3039.	5890.	4604.	6738.
<b>SEISMIC ANCHOR MOTION:</b>						
DE	1300.	871.	7515.	6155.	3834.	1151.
DDE	1690.	1152.	9519.	7782.	5161.	1463.
HOSGRI	1686.	1146.	11193.	9693.	4378.	1751.

1. Make a simple sketch of the equipment, the nozzle, the local and the global coordinate system and the north arrow in the block above. List loads in local coordinates. FA is along the nozzle centerline. Positive FA is from inside to outside of equipment.

**Figure 3. Nozzle Loads at Node 503**

**Operating Conditions**

Reference [3] defines the operating pressure conditions for the RHR line which is shown in Figure 4.



Table 9.7.2  
Reactor Coolant System Operating Pressure and Temperature Modes

<u>Line</u>	<u>Pipe Spec</u>	<u>Enveloped Conditions</u>	<u>1NN</u>	<u>2NN</u>	<u>3NN</u>	<u>3AB</u>	<u>4NB</u>
63	S6	2510	2243	2254	2504	2504	0
Note 13		650	NIS	547	579	579	NIS
109 *	S6	2510	2254	2254	2504	2504	50
Note 15			NIS	NIS	NIS	NIS	140

**Figure 4. Operating Pressures**

*(Note that the operating pressures for the RHR line are taken for line 109.)*

**RHR Suction Line Materials**

The material of the piping is ASTM A-376 TP 316 austenitic stainless steel [3]. Weld groove was installed using ER308 filler metal with 880 flux (SMAW/SAW process) [1]. For the flaw evaluation, the flow stress of the material is required. Using the design temperature of 650°F [3], the stainless steel material properties are as follows:

- Yield stress,  $\sigma_y = 18.5$  ksi [4]
- Ultimate tensile stress,  $\sigma_u = 71.8$  ksi [4]
- Flow stress,  $\sigma_f = 45.15$  ksi (average of  $\sigma_y$  and  $\sigma_u$ )

**Flaw Size**

One circumferential ID surface connected flaw was identified in the weld [3]. The flaw sketch is shown in Figure 5.

- Flaw Length at ID surface ( $2c$ ) = 4.8 inches [3]
- Flaw Depth ( $a$ ) = 0.2 inch [3]

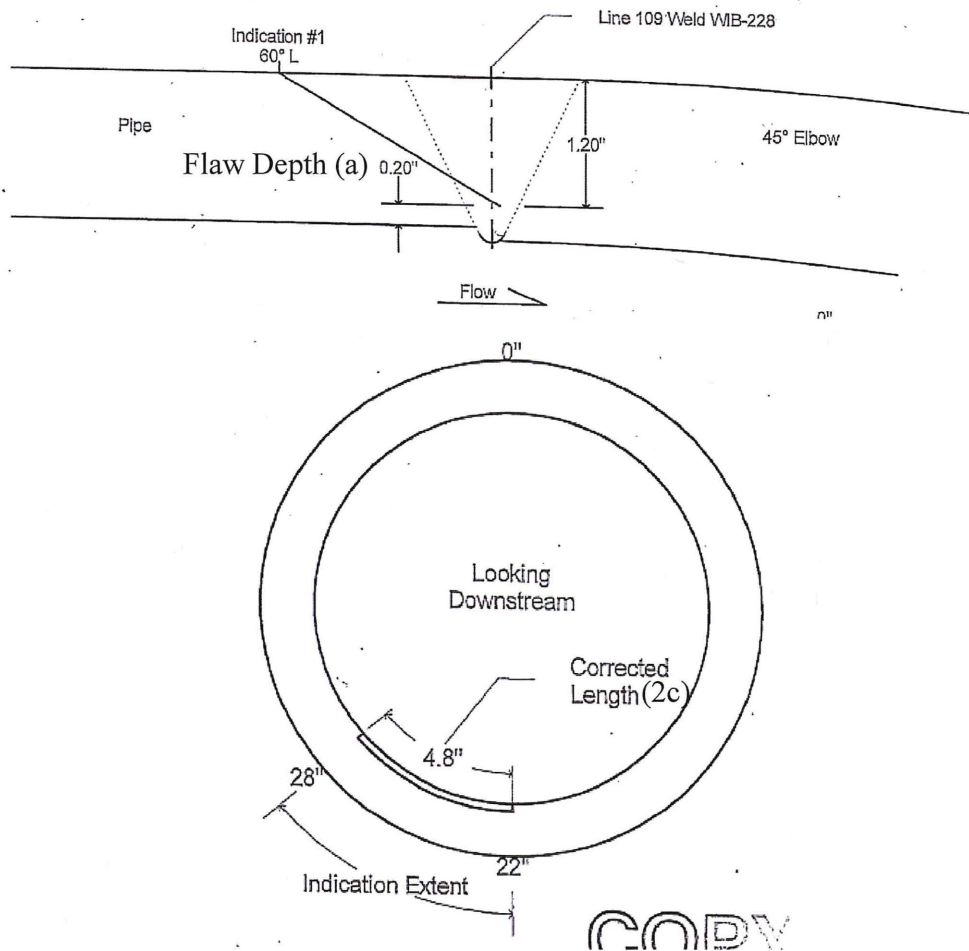


Figure 5. Flaw Configuration

**Thermal Transient**

The thermocouple data from the reactor coolant system (RCS) Loop 4 RHR piping at 100% power for Unit 2 [5] is used to perform the evaluation for Unit 1.

## ALLOWABLE FLAW SIZE DETERMINATION

The characterized flaw length is 4.8 inches with a depth of 0.2 inch [3]. The pipe wall thickness is 1.406 inches [3] resulting in a flaw depth-to-thickness ratio of 0.14. Using Table IWB-3514-2 of ASME Code Section XI [6], this flaw does not meet the Acceptance Standards and will require disposition per the flaw evaluation procedures of IWB-3600.

The stresses are calculated based on the piping loads from Reference [3]. A description of the loads is given below. After the description, the load combinations for all Service Levels are described.

- Deadweight (DW) – Deadweight of piping system, identified as DL
- Thermal (TH) – 12 thermal expansion conditions are identified as THRMN1-6 and THRMA1-6. The bounding thermal load is THRMA6, which is thermal accident load for Service Level D. THRMA6 is conservatively applied for all Service Levels to calculate allowable flaw size.
- SAM DE – Seismic anchor movements from DE condition (similar to OBE)
- SAM DD – Seismic anchor movements from DD condition (similar to SSE)
- SAM HS – Seismic anchor movements from HS condition (faulted seismic condition specific to DCPD)
- Seismic DE – Inertia seismic loads for DE condition
- Seismic DD – Inertia seismic loads from DD condition
- Seismic HS – Inertia seismic loads from HS condition

With the definition of the piping loadings, the load combinations for each Service Level are defined as:

### Primary Loads

Service Level A – DW + Pressure (P)

Service Level B – DW + P + DE

Service Level C – DW + P + DD

Service Level D – DW + P + HS

### Secondary Loads

Service Level A – TH

Service Level B – TH + SAM DE

Service Level C – TH + SAM DD

Service Level D – TH + SAM HS

The moment loads are shown in Table 1.

For the allowable flaw size evaluation, the maximum pressure for the enveloped condition, 2,510 psi shown in Figure 4, was conservatively used for all Service Levels. The applied stresses for each Service Level are shown in Table 2. The stress due to the thermal stratification, 9.964 ksi provided in Table 4, is also used to determine the allowable flaw size. The applied stresses

including the stress due to the thermal stratification transient for each Service Level are shown in Table 2.

Using the defined loading and following Section XI, Appendix C [6] EPFM guidance appropriate for the subject weld, allowable flaw sizes are calculated using **pc-CRACK** [7], a fracture mechanics program developed by Structural Integrity Associates under its quality assurance program. The allowable flaw size results are shown in Table 3.

**Table 1. Moment loading for Stress Calculations**

DW+SEIS				
Service Level	Moments, ft-lbs			Msrss, ft-lbs
	MA	MB	MC	MABC
A	1194	-1380	-1440	2325
B	3836	-3342	-4000	6494
C	4737	-4338	-5461	8446
D	7084	-5984	-8178	12389

THRMA6+SAM				
Service Level	Moments, ft-lbs			Msrss, ft-lbs
	MA	MB	MC	MABC
A	31343	-4862	-507	31722
B	37498	-8696	-1658	39064
C	39125	-10023	-1970	41174
D	41036	-9240	-2258	42501

**Table 2. Applied Stress Summary for Allowable Flaw Size Calculation**

Service Level	Pressure (psia)	$\sigma_m$ (ksi)	$\sigma_b$ (ksi)	$\sigma_e^{(1)}$ (ksi)		
				Thermal Load <sup>(2)</sup>	Thermal Stratification	Total Thermal
A	2510	6.248	0.175	2.386	9.964	12.350
B	2510	6.248	0.489	2.939	9.964	12.903
C	2510	6.248	0.635	3.097	9.964	13.061
D	2510	6.248	0.932	3.197	9.964	13.161

Notes:

- (1) The maximum membrane plus bending stress due to the thermal stratification transient, 9.964 ksi (see Table 4), is added to the secondary bending stress.
- (2) Global bending stress due to thermal expansion.

**Table 3. Allowable Flaw Size Results**

	l/circ											
	0.2	0.3	0.4	0.5	0.6	>0.75	0.2	0.3	0.4	0.5	0.6	>0.75
	Membrane + Bending						Membrane Only					
Level A	0.75	0.66	0.53	0.47	0.43	0.42	0.75	0.74	0.66	0.57	0.51	0.47
Level B	0.75	0.69	0.55	0.48	0.45	0.44	0.75	0.75	0.72	0.64	0.58	0.53
Level C	0.75	0.70	0.58	0.51	0.47	0.44	0.75	0.75	0.75	0.74	0.70	0.64
Level D	0.75	0.73	0.61	0.53	0.48	0.44	0.75	0.75	0.75	0.75	0.75	0.72
Minimum Allowable a/t	0.75	0.66	0.53	0.47	0.43	0.42	0.75	0.74	0.66	0.57	0.51	0.47

### CRACK GROWTH ANALYSIS

The crack growth analysis herein is performed using the same methodology used in the crack growth calculation for Unit 2 [8].

#### Weld Residual Stress Analysis

The residual stresses in the weld are required for the crack growth evaluation. A finite element analysis was performed to obtain the weld residual stress distribution at the RHR piping elbow weld joint using ANSYS finite element analysis software [9].

The elbow weld is performed in 8 layers. A total of 23 nuggets is defined for this weld. The weld nuggets are defined based on weld size to obtain appropriate heat penetration.

A convection heat transfer coefficient of 5.0 Btu/hr-ft<sup>2</sup>-°F at 70°F bulk ambient temperature is applied to simulate an air environment at the inside and outside surfaces during the application of the weld process. The heat generation rate for the weld, 28 kJ/in, is applied to the weld process.

After the application of the weld, a five-cycle normal operating temperature and pressure load step is appended to obtain the stabilized combined residual stresses at room temperature and also at normal operating conditions (NOC). This load step essentially simulates five heatup and cooldown ramp cycles.

The resultant residual stress distribution at room temperature is shown in Figure 6.

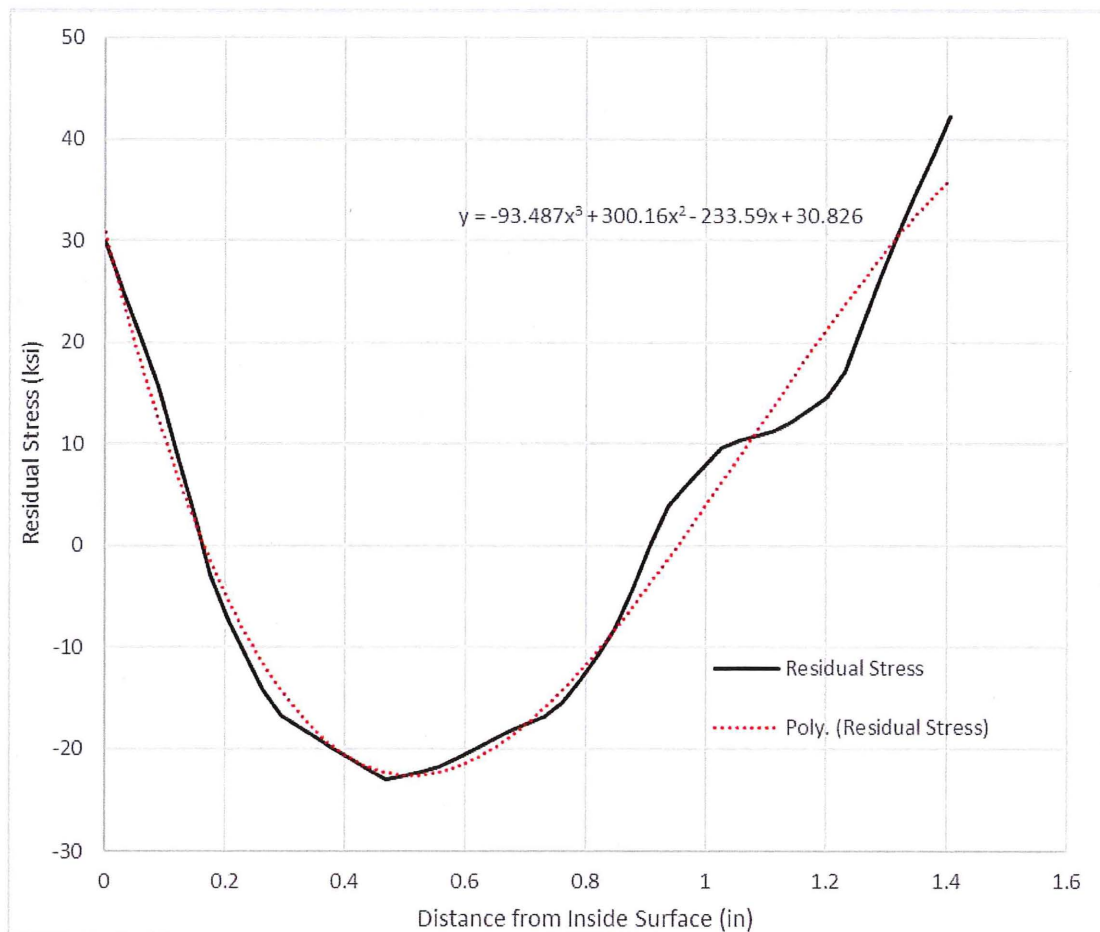


**Figure 6. Through-wall Axial Residual Stress Distribution**

### Thermal Analysis

Since the geometry of the RHR piping in Unit 1 Loop 4 is similar to the one in Unit 2 and the same thermocouple data of the RHR piping in Unit 2 is used in this analysis, the stress results of the thermal finite element analyses for Unit 2 [10] is applied in this calculation.

Linearized through-wall stresses as well as detailed through-wall stresses on a linear path through the centerline of the flaw, as shown in Figure 7, are extracted from each analysis case. The linearized membrane-plus bending ( $P_m+P_b$ ) axial stresses are compared within each analysis case to determine the maximum and minimum axial stress time points. Utilizing linearized  $P_m+P_b$  stresses is a common practice to assess the stress results within a thermal transient for fracture mechanics analysis.

The axial stress results are summarized in Table 4. The through-wall axial stresses at the corresponding minimum and maximum time points are fit into a third order polynomial. The curve fit coefficients are used in the crack growth calculation.

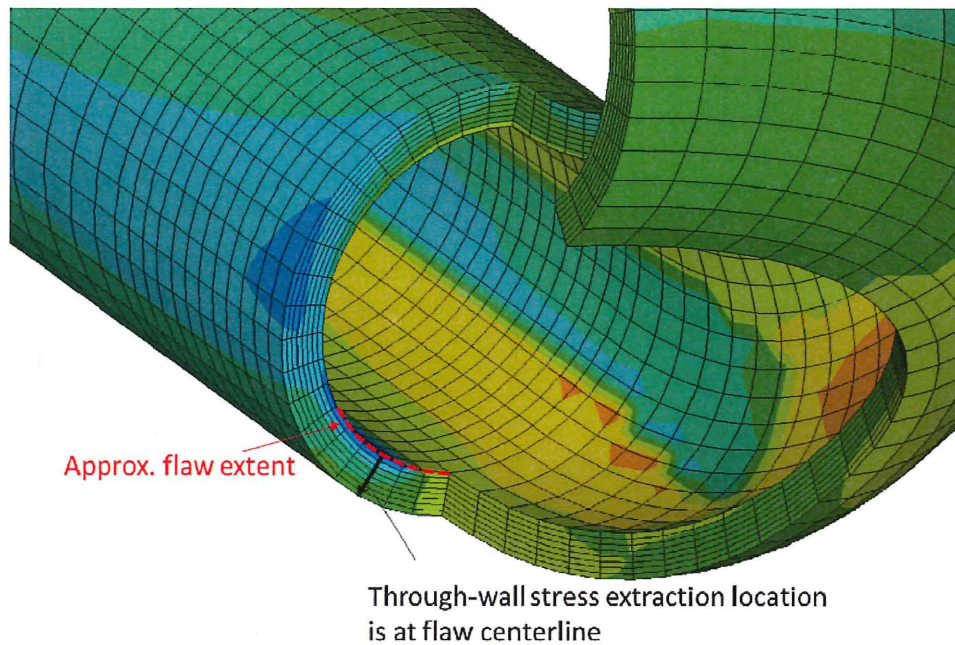


**Figure 7. Through-wall Stress Extraction Location**

**Table 4. Through-wall Axial Stress Summary for Thermal Loads**

Load Case		Linearized Stresses (ksi)		Polynomial Curve Fit Coefficients (ksi)				Quality R <sup>2</sup>
		P <sub>m</sub> +P <sub>b</sub>	P <sub>m</sub> +P <sub>b</sub>	C <sub>0</sub>	C <sub>1</sub>	C <sub>2</sub>	C <sub>3</sub>	
		(Inside)	(Outside)					
Case 1	Min	-22.602	3.283	-30.977	60.245	-42.612	10.146	0.9999
	Max	9.964	-14.044	21.232	-76.776	67.253	-19.579	0.9994
Case 2	Min	-22.609	3.281	-30.984	60.249	-42.612	10.146	0.9999
	Max	9.958	-14.045	21.225	-76.771	67.252	-19.578	0.9994
Case 3	Min	-23.724	3.161	-32.130	61.101	-42.751	10.175	0.9999
	Max	8.826	-14.155	20.047	-75.815	67.016	-19.521	0.9994
Case 4	Min	-23.733	3.158	-32.138	61.106	-42.752	10.175	0.9999
	Max	8.818	-14.158	20.039	-75.810	67.014	-19.520	0.9994
Unit Internal Pressure		1.841	1.662	1.867	-0.302	0.264	-0.111	0.9975

Cases:

1. Hot leg connection at 593°F, zero hot leg thermal anchor movement, derived RHR inside surface temperature history from TC102 to TC112 thermocouple data.
2. Hot leg connection at 607.4°F, zero hot leg thermal anchor movement, derived RHR inside surface temperature history from TC102 to TC112 thermocouple data.
3. Hot leg connection at 593°F, maximum hot leg thermal anchor movement, derived RHR inside surface temperature history from TC102 to TC112 thermocouple data.
4. Hot leg connection at 607.4°F, maximum hot leg thermal anchor movement, derived RHR inside surface temperature history from TC102 to TC112 thermocouple data.

### Stress Intensity Factors

The through-wall axial stress distributions for the internal pressure, thermal piping load, thermal stratification transient load, and weld residual stress at 70°F were input into **pc-CRACK** [7, 11].

The coefficients of third polynomial curve-fit axial stress distributions were input into **pc-CRACK**, and using “Crack Model 309 – Semi-Elliptical Circumferential Crack in Cylinder on the Inside Surface,” as shown in Figure 12 of Reference [7], the K values were determined. The stress intensity factor (K) values (as a function of crack depth) for each load cases are shown in Figure 8.

The crack model is a semi-elliptical crack in cylinder, with varying crack aspect ratio and an initial flaw depth (a) of 0.2” and an initial a half crack length (c) of 2.4”, corresponding to an aspect ratio, c/a of 12.0.

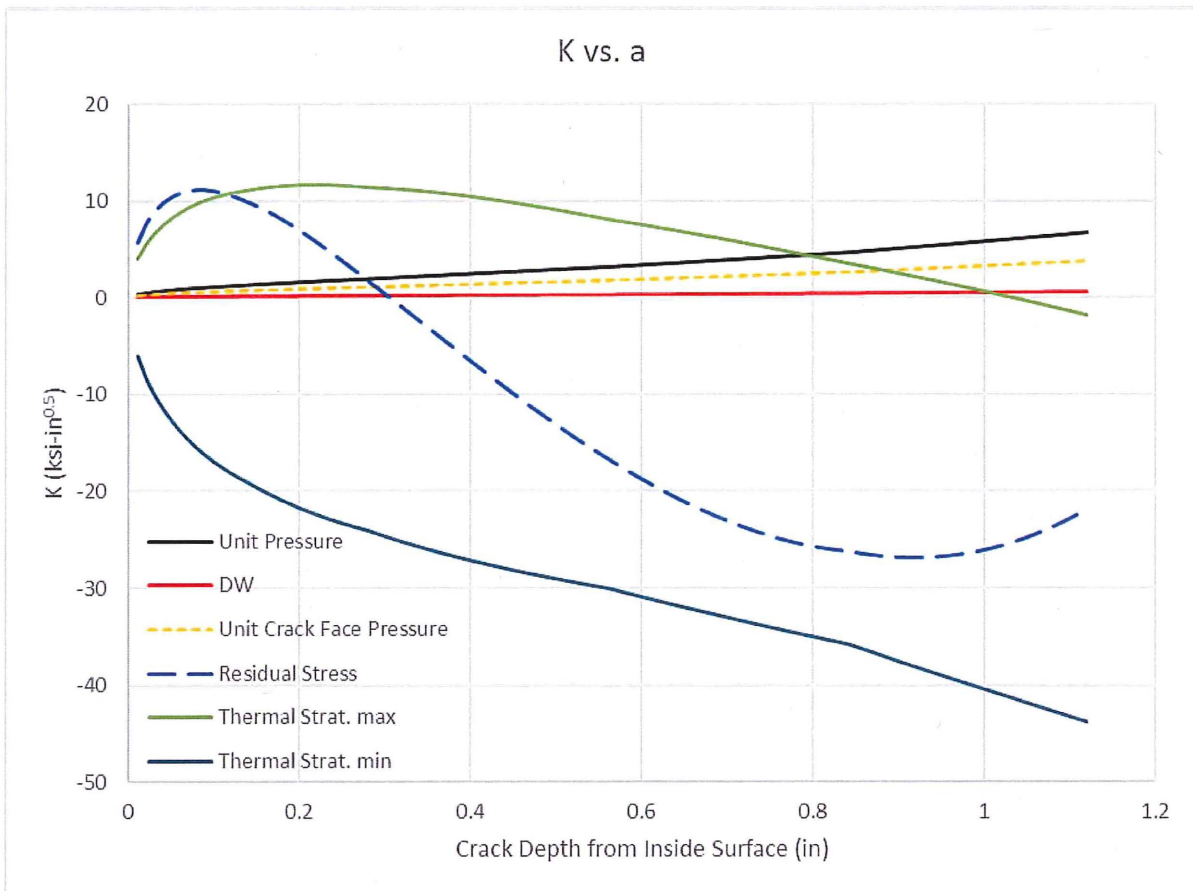


Figure 8. Stress Intensity Factors



### Fatigue Crack Growth

The FCG laws used in this analysis are discussed in the following subsections.

In FCG, the individual terms that constitute nominal  $K_{max}$  and  $K_{min}$  for the calculation of  $\Delta K$  are summarized in the following tabulations.

$K_{max}$	$K_{min}$
$K_{residual}$	$K_{residual}$
$K_{dead\ weight}$	$K_{dead\ weight}$
$K_{pressure}$	$K_{pressure}$
$K_{crack\ face\ pressure}$	$K_{crack\ face\ pressure}$
$K_{thermal\ transient\ max}$	$K_{thermal\ transient\ min}$

The individual K values for nominal  $K_{max}$  are combined (summed) with all appropriate scale factors applied. Similarly, the individual K values for nominal  $K_{min}$  are combined (summed) with all appropriate scale factors applied.  $\Delta K$  is computed by taking the difference of the resulting summed  $K_{max}$  and  $K_{min}$ . Note that  $K_{pressure}$ ,  $K_{dead\ weight}$ ,  $K_{thermal\ piping\ load}$ , and  $K_{residual}$  are constant loads during the thermal stratification transient and therefore, do not contribute to the  $\Delta K$  range. However, these K values affect the value of the R-ratio ( $K_{min}/K_{max}$ ).

The number of cycles is determined from the thermocouple data, which is discussed in Section 4.3.4 of Reference [8].

#### Fatigue Crack Growth Law for Austenitic Steels in Air

The FCG law for austenitic steels in air is per Subsubarticle C-3210 of the ASME Code, Section XI [6], as shown below, but with a multiplier of 2 [12] to account for a PWR environment.

$$da/dN = 2 \cdot C_0 (\Delta K)^n, \text{ units of inch/cycle}$$

where:

$$C_0 = C \cdot S$$

$$C = 10^{[-10.009 + 8.12 \times 10^{-4} T - 1.13 \times 10^{-6} T^2 + 1.02 \times 10^{-9} T^3]}$$

$$S = 1.0 \text{ when } R \leq 0$$

$$= 1.0 + 1.8R \text{ when } 0 < R \leq 0.79$$

$$= -43.35 + 57.97R \text{ when } 0.79 < R < 1.0$$

$$T = \text{metal temperature, } ^\circ\text{F (taken as the average fluid temperature during the transient)}$$

$$R = K_{min}/K_{max} = \text{R-ratio}$$

$$\Delta K = K_{max} - K_{min} \text{ (range of applied K), ksi}\sqrt{\text{in}}$$

$$n = 3.3 \text{ per Section XI, Appendix C [6]}$$

#### Fatigue Crack Growth Law using Code Case N-809 Equation

The FCG law for Type 304 and Type 316 stainless steels and associated weld metals from ASME Code Case N-809 [13] is also considered in order to compare the results of the FCG law shown above.

$$da/dN = C_0 \cdot \Delta K^n, \text{ units of inch/cycle}$$

where:

- $C_0$  = scaling parameter that accounts for the effect of loading rate and environment on fatigue crack growth rate  
 $= C S_T S_R S_{ENV}$
- $n$  = slope of the log (da/dN) versus log ( $\Delta K$ ) curve = 2.25
- $C$  = nominal fatigue crack growth rate constant  
 $= 4.43 \times 10^{-7}$  for  $\Delta K \geq \Delta K_{th}$   
 $= 0$  for  $\Delta K < \Delta K_{th}$
- $\Delta K$  = stress intensity factor range, ksi $\sqrt{in}$   
 $\Delta K_{th}$  = 1.10 ksi $\sqrt{in}$
- $S_T$  = parameter defining effect of temperature on FCG rate  
 $= e^{-2516/T_K}$  for  $300^\circ F \leq T \leq 650^\circ F$   
 $= 3.39 \times 10^5 e^{[-(2516/T_K) - 0.0301T_K]}$  for  $70^\circ F \leq T < 300^\circ F$
- $T$  = metal temperature,  $^\circ F$
- $S_R$  = parameter defining the effect of R-ratio on FCG rate  
 $= 1.0$  for  $R < 0$   
 $= 1 + e^{8.02(R-0.748)}$  for  $0 \leq R < 1.0$
- $R$  =  $K_{min}/K_{max}$  = R ratio
- $S_{ENV}$  = parameter defining the environmental effects on FCG rate  
 $= T_R^{0.3}$
- $T_R$  = loading rise time, sec
- $T_K$  =  $[(T-32)/1.8+273.15]$ , K

### Stress Corrosion Crack Growth

SCC is a time dependent phenomenon and occurs during sustained loading conditions. Given that the great majority of plant operation is at steady state normal operating conditions (NOC), SCC is defined by the stress condition at NOC. SCC is defined to be active when the K at steady state NOC is a positive number. If SCC is active, crack growth is determined for one-month time period. Alternating one-month blocks (periods) of FCG and SCC growth (if SCC is active) are used to calculate total cumulative crack growth.

Even though the stress due to the thermal stratification is cyclic in nature, the frequency is high enough that the maximum thermal stratification stress is treated as a constant stress in the SCC growth evaluation.

For SCC, the K is calculated in the following tabulation.

K
K <sub>residual</sub>
K <sub>pressure</sub>
K <sub>crack face pressure</sub>
K <sub>deadweight</sub>
K <sub>thermal transient max</sub>

### SCC Growth Law

The SCC growth law for the Type 304 stainless steel is taken from BWRVIP-14-A [14]. Note that the use of this equation for the evaluation of Type 316 weld is conservative since Type 316 austenitic stainless steel is more resistant to IGSCC.

$$\ln\left(\frac{da}{dt}\right) = 2.181 \ln(K) - 0.787 \text{ Cond}^{-0.586} + 0.00362 \text{ ECP} + \frac{6730}{T_{\text{ABS}}} - 33.235$$

where:

da/dt	=	crack growth rate (change in crack depth per unit time), mm/s
K	=	stress intensity, MPa√m
Cond	=	average conductivity (determined at room temperature), μS/cm
ECP	=	electrochemical corrosion potential, mV(SHE)
SHE	=	Standard Hydrogen Electrode
T <sub>ABS</sub>	=	temperature, K

The above crack growth equation is converted to following simpler K-dependent form:

$$\frac{da}{dt} = CK^n$$

where,

da/dt	=	crack growth rate, inch/hour
C, n	=	material constants
K	=	stress intensity factor, ksi√in

A metal temperature of 450°F is applied to calculate the material constants, C and n. The calculated constants,  $C = 2.42 \times 10^{-7}$  and  $n = 2.181$ , are applied to calculate SCC growth. No stress corrosion crack growth threshold is considered.

### **Results of Analysis**

The crack growth results are shown in Figure 9. The allowable flaw size is calculated based on the  $l/circumference$  at each crack depth since the  $l/circumference$  is also changed for every month as shown in Figure 10. At the weld location, it takes 41 months for the initial flaw of 0.2 inches to reach the allowable flaw size when ASME Code FCG equation is used. It takes 35 months for the initial flaw of 0.2 inches to reach the allowable flaw size when Code Case N-809 FCG equation is used. Table 7 shows the monthly crack growth per FCG and SCC.

**Table 7. Monthly Crack Growth**

Time (Month)		Crack Depth (in)	
		ASME Code Eq. Austenitic Steel in Air	Code Case N-809
0		0.2000	0.2000
1	FCG	0.2520	0.2982
	SCC	0.3486	0.3706
2	FCG	0.4028	0.4626
	SCC	0.4305	0.4735
3	FCG	0.4788	0.5355
	SCC	0.4869	0.5368
4	FCG	0.5302	0.5796
	SCC	0.5320	0.5796
5	FCG	0.5653	0.5877
	SCC	0.5655	0.5877
6	FCG	0.5882	0.5917
	SCC	0.5882	0.5917
12	FCG	0.6075	0.6125
	SCC	0.6075	0.6125
24	FCG	0.6290	0.6328
	SCC	0.6290	0.6328
35	FCG	0.6358	0.6357
	SCC	0.6358	0.6357
41	FCG	0.6358	-
	SCC	0.6358	-

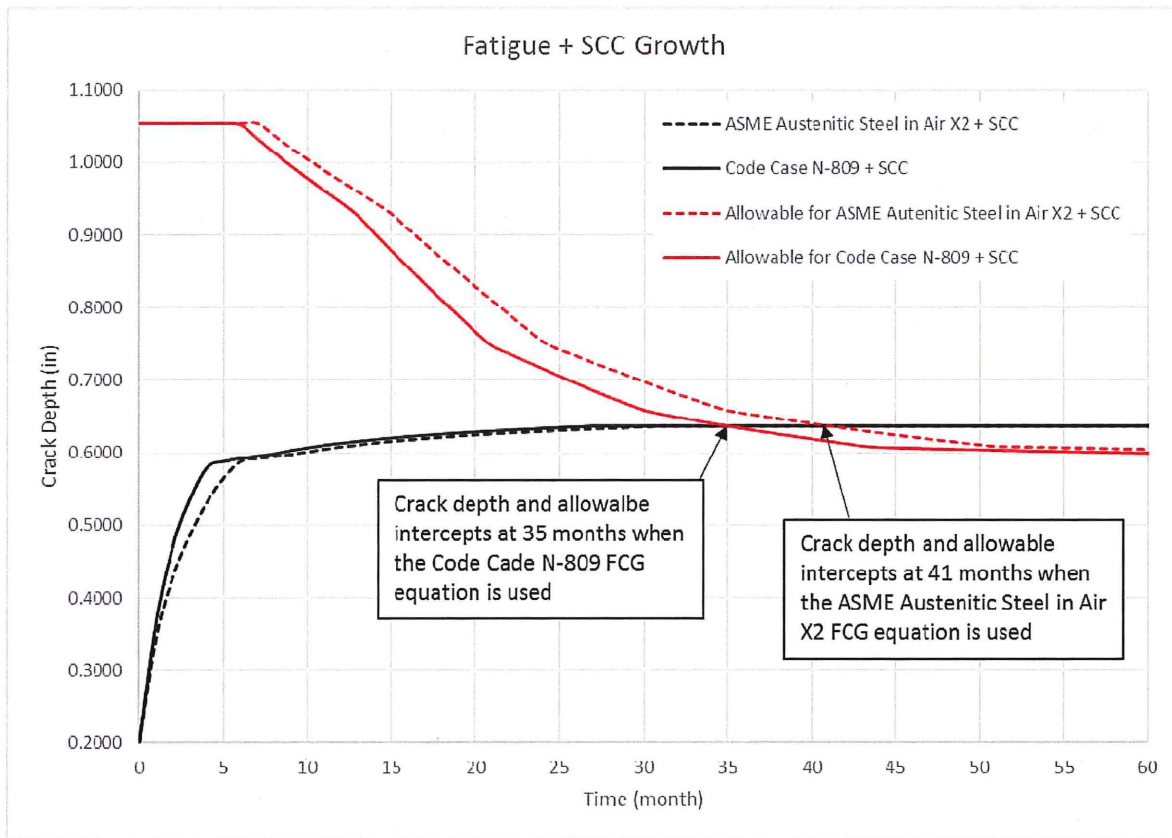


Figure 9. Fatigue plus SCC Growth Results from an Initial Flaw Size of 0.2 in

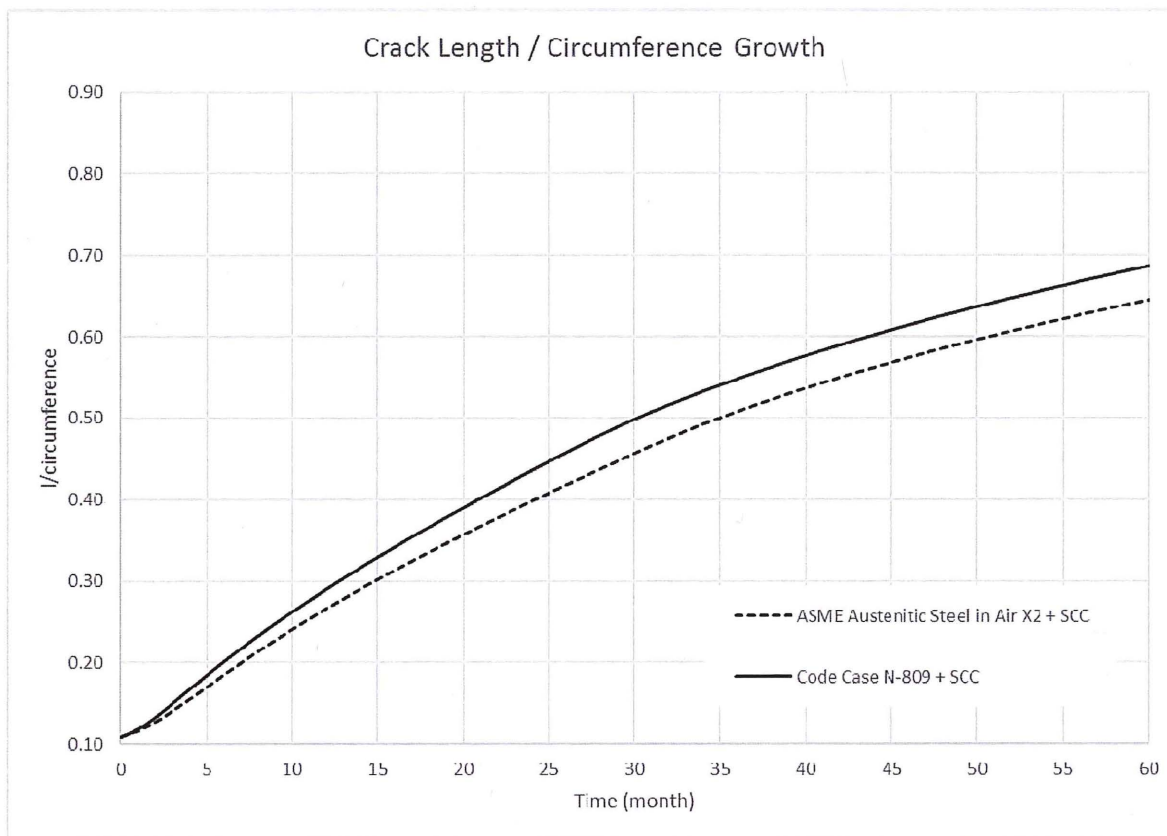


Figure 10. Crack Length per Circumference Growth Results

## CONCLUSIONS

The evaluation herein determines allowable flaw depths and expected crack growth for the RHR suction line at DCP, Unit 1 where cracking was recently discovered. The cracking is located in the pipe-to-45° elbow weld (WIB-228). Using the methods of ASME Section XI, Appendix C, allowable flaw depth at the crack location was determined as a function of flaw length-to-circumference ratio.

The evaluation for Unit 2 [2] was performed according to the ASME Section XI 2001 Edition through 2003 Addenda [6]. In this report, the analytical evaluation that was performed for Unit 2 was replicated using the flaw parameters, pipe dimensions, and loads that were applicable to Unit 1, since the configuration of the pipe/weld, materials, operation and load history are similar for both Units 1 and 2. However, the applicable ASME Section XI Code of reference for Unit 1 is 2007 Edition through 2008 Addenda [16]. The methodology and criteria to perform the flaw evaluation herein using ASME Code Section XI “2001 Edition through 2003 Addenda [6]” and “2007 Edition through 2008 Addenda [16]” are identical and the material properties are the same for both the Code Editions [References 4 and 17]. The Code Edition has no impact on the analytical results.

Fatigue and SCC growth analyses has been performed for the flaw at WIB-228 because the exact root cause of the cracking is not confirmed. Vibration was not included since it was ruled out as a possible cause. Temperature data collected along the similarly affected RHR suction line for Unit 2, which shows significant thermal stratification cycling near the location of the identified flaw, has been used to perform the flaw evaluation for Unit 1.

The results show that at the weld location, it would take 35 months for the initial flaw of 0.2 inch to reach the allowable flaw size. The results indicate that FCG is the predominant contributor to crack growth and while the presence of SCC is considered unlikely, it is conservatively included for the purposes of this evaluation.

Thus, based on the crack growth rates presented in this report, the flaw in the 45° elbow weld of the RHR suction line at DCPD, Unit 1 is acceptable for continued operation until the 1R21 refueling outage which will not exceed a two-year duration.

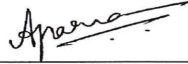
## REFERENCES

1. SI Calculation No. 1600539.301, Rev. 0, "Evaluation of the Flaw in the RHR Suction Weld Joint."
2. SI Report No. 1600539.401, Rev. 0, "Flaw Evaluation of RHR Suction Weld Joint Final Report at Diablo Canyon Power Plant, Unit 2."
3. DCPD Design Input Transmittal No. DIT-50915871-001-00, "Unit 1 RHR suction line loads and configuration," SI File No. 1700609.206.
4. ASME Boiler and Pressure Vessel Code, Section II, Part D - Material Properties, 2001 Edition, with Addenda through 2003.
5. DCPD Design Input Transmittal No. DIT-50852155-003-02, "2R19 RHR Suction Weld Joint Flaw Evaluation," SI File No. 1600539.211.
6. ASME Boiler and Pressure Vessel Code, Section XI, 2001 Edition, with Addenda through 2003.
7. **pc-CRACK** 4.1 CS, Version Control No. 4.1.0.0, Structural Integrity Associates, December 31, 2013.
8. SI Calculation No. 1600539.304, Rev. 0, "Crack Growth Evaluation in the RHR Suction Weld Joint."
9. ANSYS Mechanical APDL, Release 14.5 (w/ Service Pack 1 UP20120918), ANSYS, Inc., September 2012.
10. SI Calculation No. 1600539.303, Rev. 0, "Finite Element Stress Analysis of the RHR Piping."
11. SI V&V Report No. 1700609.301, Rev. 0, "Verification of pc-CRACK 4.2 output."
12. Section XI Task group for Piping Flaw Evaluation, ASME Code, the Journal of Pressure Vessel Technology, "Evaluation of Flaws in Austenitic Piping" Volume 108, Number 3, dated August 1986.
13. ASME Code Case N-809, "Reference Fatigue Crack Growth Rate Curves for Austenitic Stainless Steels in Pressurized Water Reactor Environments Section XI, Division 1," Cases the ASME Boiler and Pressure Vessel Code, June 23, 2015.

14. BWRVIP-14-A: BWR Vessel and Internals Projects, Evaluation of Crack Growth in BWR Stainless Steel RPV Internals, EPRI, Palo Alto, CA: 2008. 1016569.
15. Email from Mark Sharp (PG&E) to Aparna Alleshwaram (SI), "CONFIDENTIAL: Initial EI 50915871 - OM7.ID7 Problem Statement - Indication found using UT at weld WIB-228," dated 4/28/2017, SI File No. 1700609.201.
16. ASME Boiler and Pressure Vessel Code, Section XI, 2007 Edition, with Addenda through 2008.
17. ASME Boiler and Pressure Vessel Code, Section II, Part D - Material Properties, 2007 Edition, with Addenda through 2008.



Prepared by:




\_\_\_\_\_  
Aparna Alleshwaram  
Senior Consultant

08/04/17

\_\_\_\_\_  
Date

Checked by:

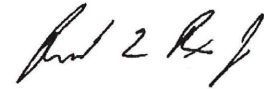


\_\_\_\_\_  
Stan Tang  
Associate

08/04/17

\_\_\_\_\_  
Date

Verified by:



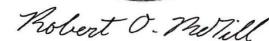
\_\_\_\_\_  
Richard Bax signing on  
behalf of D. J. Shim  
D. J. Shim  
Associate

08/04/17

\_\_\_\_\_  
Date

Approved by:





\_\_\_\_\_  
Robert McGill, P.E.  
Senior Associate

08/04/17

\_\_\_\_\_  
Date